ELSEVIER

Journal of Nuclear Materials 273 (1999) 315–325

journal of nuclear materials

www.elsevier.nl/locate/jnucmat

Influence of prior thermal ageing on tensile deformation and fracture behaviour of forged thick section 9Cr–1Mo ferritic steel

B.K. Choudhary [a], K. Bhanu Sankara Rao [a], S.L. Mannan [a,*], B.P. Kashyap [b]

[a] *Materials Development Division, Indira Gandhi Centre for Atomic Research, Kalpakkam 603 102, India*
[b] *Department of Metallurgical Engineering and Materials Science, I.I.T., Bombay 400 076, India*

Received 13 October 1998; accepted 29 January 1999

Abstract

Tensile tests were performed on specimens in quenched and tempered (Q + T) and thermally aged (TA) conditions over a wide temperature range (300–873 K) to assess the influence of prior thermal ageing on tensile deformation and fracture behaviour of forged thick section 9Cr–1Mo ferritic steel. Prior thermal ageing at 793 and 873 K for durations ranging from 10 to 5000 h did not cause a significant change in room temperature tensile properties. However, a marginal decrease in yield strength and reduction in area were observed for specimens aged for longer durations at 793 and 873 K. Prior thermal ageing at 793 K for 5000 h and at 873 K for 1000 and 5000 h produced significant reduction in strength values at intermediate temperatures (523–723 K) compared to that observed at high temperatures. At intermediate temperatures, the alloy in all heat treatment conditions exhibited serrated flow, a manifestation of dynamic strain ageing (DSA). The significant loss of strength in thermally aged conditions at intermediate temperatures has been attributed to reduced propensity to DSA. The elongation to fracture values at temperatures in the range 300–873 K were affected little by prior thermal ageing, whereas the reduction in area exhibited a decrease in the value with increasing thermal ageing. The fracture mode remained transgranular ductile at all test conditions investigated in the present study. However, specimens aged for longer durations exhibited chisel fracture at room and intermediate temperatures due to split in the martensite lath boundaries. The influence of thermal ageing on room temperature tensile properties of the forging remained similar to that reported for thin section 9Cr–1Mo steel. © 1999 Elsevier Science B.V. All rights reserved.

1. Introduction

Ferritic steel, 9Cr–1Mo and its modified versions are important candidate materials for thick section tube plates and tubings for steam generators of liquid metal cooled fast breeder reactors (LMFBRs). The selection of 9Cr–1Mo steel for steam generator applications in LMFBRs is based on the low thermal expansion coefficient and high resistance to stress corrosion cracking in water–steam systems, in addition to better mechanical properties at elevated temperatures compared to alternate 2 1/4Cr–1Mo steel. The good weldability and good microstructural stability over long time exposure at elevated temperatures are other attractive features that have favoured the selection of 9Cr–1Mo steel for steam generator applications. The mechanical properties (tensile, creep and creep-fatigue) of 9Cr–1Mo steel in the normalised and tempered condition have been reliably established for thin sections [1–4]. The potential of 9Cr–1Mo steel for use in thick sections has been assessed by conducting tension and strain-controlled low-cycle fatigue tests on bar stock material subjected to heat treatments intended to simulate thick sections [5,6]. In view of the paucity of information on the elevated-temperature mechanical properties of forged thick section, an extensive test programme was undertaken to

* Corresponding author. Tel.: +91-4114 40222; fax: +91-4114 40360; e-mail: mannan@igcar.ernet.in

0022-3115/99/$ – see front matter © 1999 Elsevier Science B.V. All rights reserved.
PII: S0022-3115(99)00051-3

evaluate tensile, creep, low cycle fatigue and creep-fatigue behaviour of 1000 mm diameter and 300 mm thick forged tube plate of 9Cr–1Mo steel [7]. Materials during service at high temperatures undergo thermal ageing resulting in microstructural degradation, which in turn influences the mechanical properties. Therefore, investigations were conducted to assess the influence of prior thermal ageing on tensile deformation and fracture behaviour of this steel.

The variation of yield and ultimate tensile strengths of normalised and tempered thin section 9Cr–1Mo steel with temperature exhibit a gradual decrease from ambient to an intermediate temperature followed by a rapid decrease at high temperatures [2]. Elongation to fracture decreases with increase in temperature to 773 K, whereas reduction in area shows a marginal decrease in this temperature range. At high temperatures, both the values show a rapid increase with increasing temperature. Detailed investigation on the influence of strain rate and temperature on the tensile properties of the forging in the simulated post weld heat treatment condition indicated similar behaviour [7,8]. However, the strength values of the forging were found to be lower than that of thin section in the normalised and tempered condition [2] and in the heat treatment conditions intended to simulated thick sections [5,6]. The lower strength values of the forging have been attributed to its coarse grain size and coarse lath martensite [7,8]. The tensile ductility of the forging was higher than that of thin section. Further, the alloy exhibited serrated flow, negative strain rate sensitivity, ductility minima and anomalies in the variation of work hardening parameters associated with stress–strain relationship with temperature and strain rate at intermediate temperatures [7–9]. A recent investigation [10] on a wide range of simulated heat affected zone microstructures indicated that the intercritical microstructure possesses the lowest strength, whereas coarse grain microstructure having fine lath martensite displays the highest strength coupled with low tensile ductility. The fine grain structure exhibits a good combination of strength and ductility, and hence, it is desirable in 9Cr–1Mo steel.

Subjecting the alloy to thermal ageing at 773 and 823 K causes no significant variation in the strength values at ambient temperatures [11–14]. However, thermal ageing for longer durations caused a loss of ductility [11–14] and inferior impact properties [11]. Wall et al. [11] observed a ductility trough and mixed ductile/brittle intergranular fracture at room temperature in the alloy subjected to thermal ageing at 823 K. Hippsley and Haworth [12] reported transgranular fracture characterized by dimples resulting from microvoid coalescence in the normalised and tempered condition and chisel fracture in the thermally aged condition. The reduced tensile ductility at room temperature in thermally aged thin section 9Cr–1Mo steel has been attributed to the change in the nucleation and growth characteristics of voids at both inclusions and fine precipitates due to a combination of phosphorous segregation at precipitate-matrix interfaces and the precipitation of Laves phase, Fe_2Mo [13,14]. Little information is available on the influence of thermal ageing on the elevated temperature tensile properties of this alloy. Present investigation is aimed at evaluating and understanding the influence of thermal ageing on tensile behaviour of forged thick section 9Cr–1Mo steel over a wide temperature range. It is also aimed at examining the applicability of information available on thermally aged thin sections to thick section 9Cr–1Mo steel.

2. Experimental

2.1. Test material and tensile testing

The test material, a nuclear grade 9Cr–1Mo ferritic steel tube plate forging of 1000 mm diameter and 300 mm thickness was supplied by BRUCK GmbH, Germany. The chemical composition is given in Table 1. The hot forged tube plate was austenitized followed by quenching and then tempering (Q + T). The austenitizing treatment consisted of controlled heating (heating time 8 h) to 1223 K and soaking at 1223 K for 5 h followed by quenching in water. The tempering treatment involved controlled heating (heating time 8 h) to 1023 K and soaking at 1023 K for 8 h followed by air cooling. Specimen blanks of 12 mm diameter and 60 mm length were machined from the outer annulus of 300 mm width of the forging. These blanks were machined with stress axis in the thickness direction of the forging. Some batches of Q + T specimen blanks were thermally aged (TA) at 793 and 873 K for durations in the range 10–5000 h.

Following the heat treatments, cylindrical button head tensile specimens with a gauge diameter of 4 mm and gauge length of 26 mm were machined from the blanks. Tensile tests were carried out in air in a floor model Instron 1195 universal testing machine equipped

Table 1
Chemical composition of 9Cr–1Mo steel forging

Element	C	Si	Mn	S	P	Cu	Ni	Cr	Mo	N	Fe
Amount (wt%)	0.10	0.75	0.63	0.001	0.02	1.00	1.12	9.27	1.05	190 (ppm)	Balance

with a three-zone temperature control furnace and a stepped-load suppression unit. Tests were performed on Q + T specimens over a temperature range 300–873 K at a nominal strain rate of 1.3×10^{-3} s^{-1}. Specimens aged at 793 K for various durations of 10, 50, 100, 500 and 1000 h and at 873 K for durations 10, 50, 100 and 500 h were tested at room temperature, whereas specimens aged at 793 K for 5000 h and at 873 K for 1000 and 5000 h were tested in the temperature range 300–873 K. Temperature in all the tests were controlled within ±2 K. Load-elongation curves were recorded using the Instron autographic recorder for all the tests. Use of suitable chart speed gave a strain resolution of 7.5×10^{-4} and stepped zero suppression gave a stress resolution of 0.80 MPa.

2.2. Metallography

Optical metallographic examinations on Q + T and thermally aged specimens were carried out in a Reichert MeF_2 optical microscope equipped with a camera. Specimens were prepared using standard metallographic techniques and by immersion etching in Vilella's reagent (1 g picric acid + 5 ml HCl + 100 ml ethyl alcohol). Fractographic examinations on tested specimens were carried out using PSEM 501 scanning electron microscope (SEM).

2.3. Precipitate extraction and analysis

In order to identify the type of precipitate present in the as-received Q + T and thermally aged specimens, selective extraction of precipitates was carried out by electrochemical extraction technique using a 3–4 g sample as an anode and 10% HCl in alcohol as electrolyte. A potential of 1.5 V with respect to a platinum cathode resulted in the selective dissolution of the matrix, thus enabling the precipitate extraction. The extracted precipitates were separated by alternate centrifuging and washing by alcohol. After drying, the total weight percent was determined. Precipitates were identified by X-ray diffraction analysis of the precipitates using Cu–Kα ($\lambda = 1.542$ Å) radiation.

3. Results and discussion

3.1. Microstructure

The microstructures obtained at the end of quenching and tempering and thermal ageing treatments are shown in optical micrographs in Figs. 1–3. In the Q + T condition, the microstructure was composed of tempered lath martensite and a few stringers of proeutectoid ferrite (α-Fe) at the prior austenite grain boundaries (Fig. 1(a)). An average value of proeutectoid ferrite of

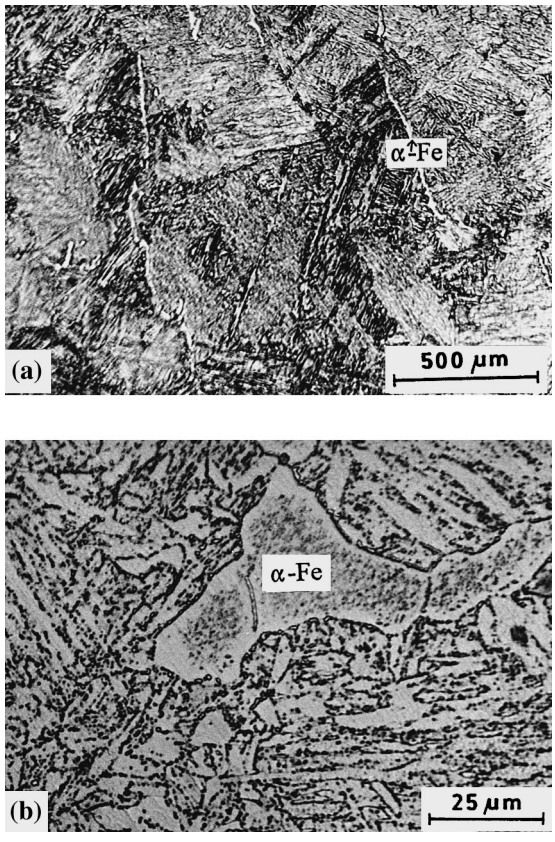

Fig. 1. Microstructure of the forging in Q + T condition showing: (a), Lath martensite and proeutectoid ferrite (α-Fe); (b), Tempered lath martensite and proeutectoid ferrite exhibiting coarse precipitates on grain and lath boundaries and fine precipitates in the intragranular and intralath regions.

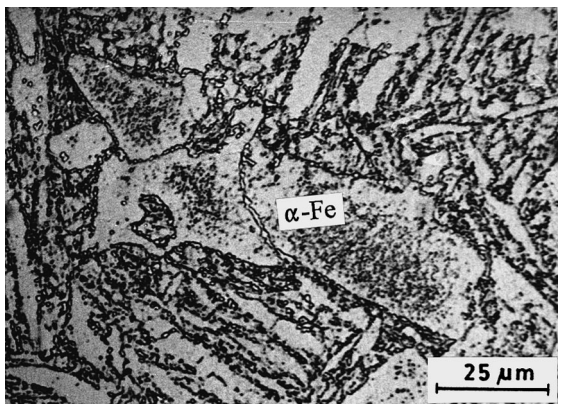

Fig. 2. Microstructure of the alloy after thermal ageing at 793 K for 5000 h showing coarser precipitates in the lath martensite and proeutectoid ferrite boundaries and in the matrix.

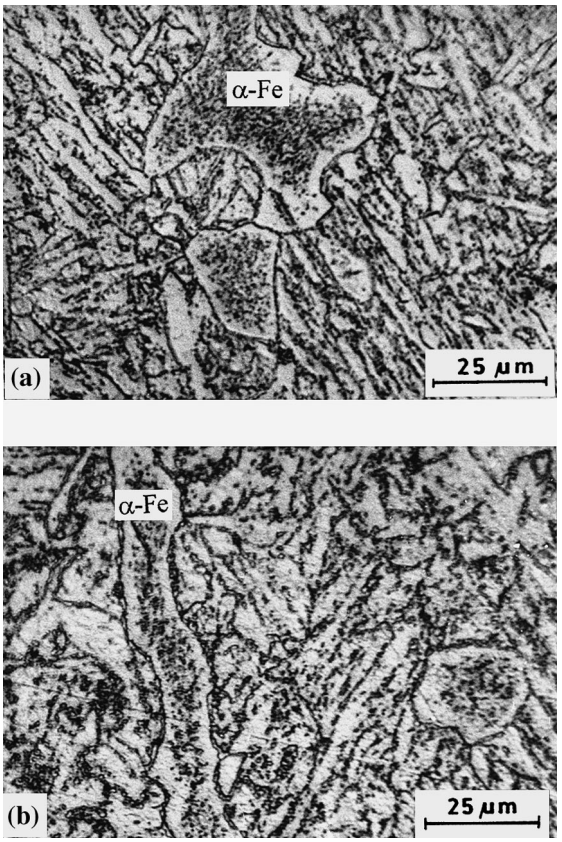

Fig. 3. Microstructure of the alloy after thermal ageing at 873 K for: (a), 1000 and (b), 5000 h showing coarser precipitates in the lath martensite and proeutectoid ferrite boundaries and in the matrix.

~2% was estimated by the point count method in the regions of machining of specimens. The prior austenite grain size of the tube plate forging characterized by mean linear intercept was 120 μm. The boundaries of prior austenite grains, martensite laths and proeutectoid ferrite were decorated with various precipitates (Fig. 1(b)). The intralath matrix and the proeutectoid ferrite regions contained a large number of fine precipitates. Subjecting the alloy to thermal ageing at 793 and 823 K for longer durations (e.g., at 793 K for 5000 h in Fig. 2 and at 873 K for 1000 and 5000 h in Fig. 3), the basic microstructure remained similar to that of Q + T condition. However, the precipitates on prior austenite, lath martensite and proeutectoid ferrite boundaries coarsened, and additional precipitation took place in the intralath and within the proeutectoid ferrite regions (Figs. 2 and 3).

A tempered martensite structure has been reported in normalised and tempered thin sections and after heat treatments aimed at simulating the microstructure of thick sections of plain 9Cr–1Mo steel [1,4–6]. Tempered lath martensitic structure has been also reported in normalised and tempered modified 9Cr–1Mo steel [15,16]. The presence of about 2% proeutectiod ferrite in the microstructure observed in the present investigation appears to have resulted from the slower cooling rate experienced by the forging due to its large section size. The coarse prior austenite grain size of 120 μm of the forging compared to 20–30 μm for thin section hot rolled material austenitized in the temperature range 1223–1273 K [1,4] could have resulted from the high hot forging temperature [16] and the extended heat treatment comprised of slow heating to the austenitizing temperature and higher soaking time of 5 h employed on the forging.

The variation of total weight percent of bulk precipitates with thermal ageing is shown in Fig. 4. Specimens for ageing durations longer than 5000 h were taken from the shoulder region of creep specimens tested at 793 and 873 K [7]. The weight percent of precipitates obtained on specimens subjected to an additional heat treatment of simulated post weld heat treatment (SPWHT) [8] is also given in Fig. 4. The weight percent of precipitates increased marginally due to thermal ageing at 793 K up to 1000 h followed by a rapid increase at longer ageing durations. At the higher ageing temperature of 873 K, the onset of a rapid increase in precipitation was observed at 500–2200 h, followed by a nearly constant value at longer times. The earlier onset of rapid increase in the bulk precipitates at 873 K than that observed at 793 K can be ascribed to the faster kinetics of precipitation. X-ray diffraction analysis of the bulk precipitates detected the presence of $M_{23}C_6$ ($\{Cr\ Fe\}_{23}C_6$) and M_2X (Cr_2N) in all the specimens. The above observations are in agreement with earlier investigations [4,11–14,17]. An X-ray peak corresponding to intermetallic Laves phase (Fe_2Mo) was observed at 873 K aged for durations of 12 570 h and above. Based on transmission electron microscopy investigations on carbon extraction replicas, Wall et al. [11], Hippsley and Haworth [12] and Senior et al. [13,14] reported Laves

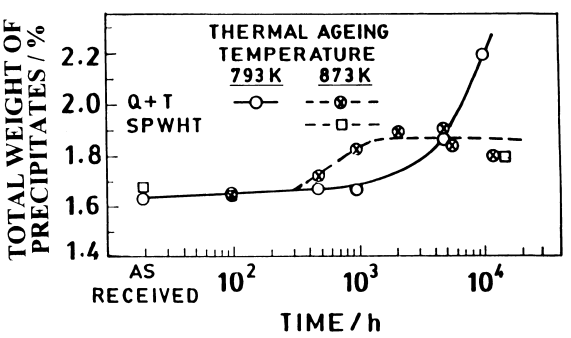

Fig. 4. Variation of total weight percent of precipitates as a function of thermal ageing duration at 793 and 873 K.

phase (Fe_2Mo) formation after thermal ageing for 1000 h in the temperature range 773–823 K. Increased weight percent of bulk precipitate in the thermally aged specimens is in agreement with the observation of Brinkman et al. [15] in the modified 9Cr–1Mo steel thermally aged in the temperature range 755–811 K.

3.2. Tensile properties

Room temperature tensile properties and hardness values of 9Cr–1Mo steel in Q + T and thermally aged conditions are presented in Figs. 5 and 6. A minimum of two tests on Q + T and thermally aged specimens were conducted at room temperature and the average value has been reported in these figures. The ultimate tensile strength values were little affected by prior thermal ageing at 793 and 873 K for durations 10–5000 h. Specimens thermally aged for longer durations at both temperatures exhibited a marginal decrease in yield strength values. However, hardness values of thermally aged specimens exhibited some decrease compared to that of Q + T specimens. The uniform plastic elongation and total elongation remained similar to that of Q + T specimens. Reduction in area of the aged specimens

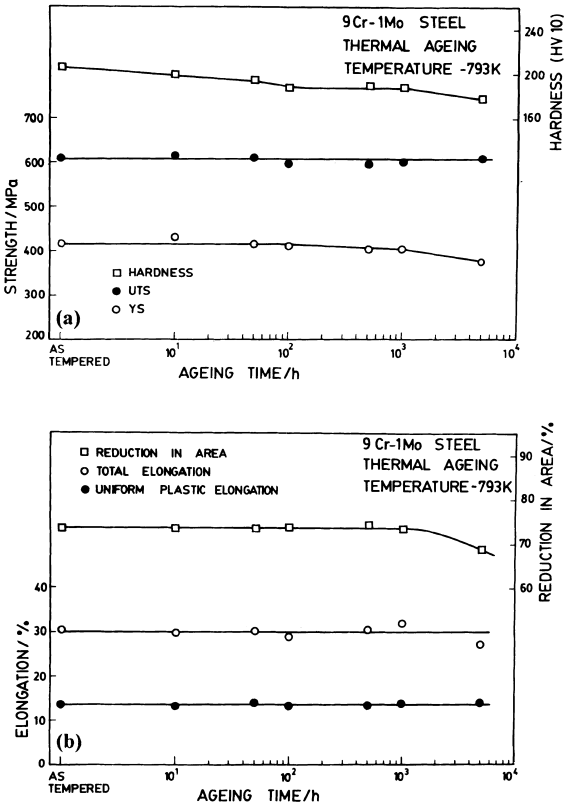

Fig. 5. Influence of prior thermal ageing at 793 K on room temperature mechanical properties of 9Cr–1Mo steel.

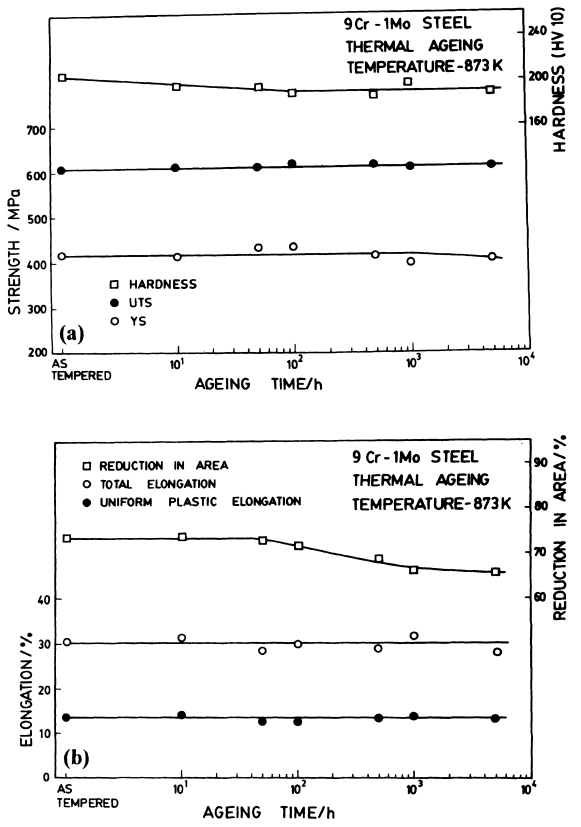

Fig. 6. Influence of prior thermal ageing at 873 K on room temperature mechanical properties of 9Cr–1Mo steel.

exhibited a decrease after longer ageing times (Fig. 5(b) and Fig. 6(b)). The decrease in reduction in area was more pronounced in specimens aged at 873 K (Fig. 6(b)).

The variation in yield strength and ultimate tensile strength of Q + T and thermally aged (i.e., at 793 K for 5000 h and at 873 K for 1000 and 5000 h) specimens with temperature are shown in Figs. 7 and 8, respectively. Both the strength values decreased gradually with increasing temperature up to an intermediate temperature followed by a rapid decrease at high temperatures. Prior thermal ageing at 793 K for 5000 h and at 873 K for 1000 and 5000 h indicated significant influence on the strength values at intermediate and high temperatures (Figs. 7 and 8). A maximum reduction in strength values due to thermal ageing was observed at intermediate temperatures, where serrated flow was noticed. The decrease in strength values was more pronounced in yield strength than in ultimate tensile strength. The elongation to fracture values for specimens thermally aged for longer durations were found to lie within ±20% scatter band for Q + T specimens at all temperatures (Fig. 9). The reduction in area exhibited a consistent decrease with increase in thermal ageing (Fig. 10). Also,

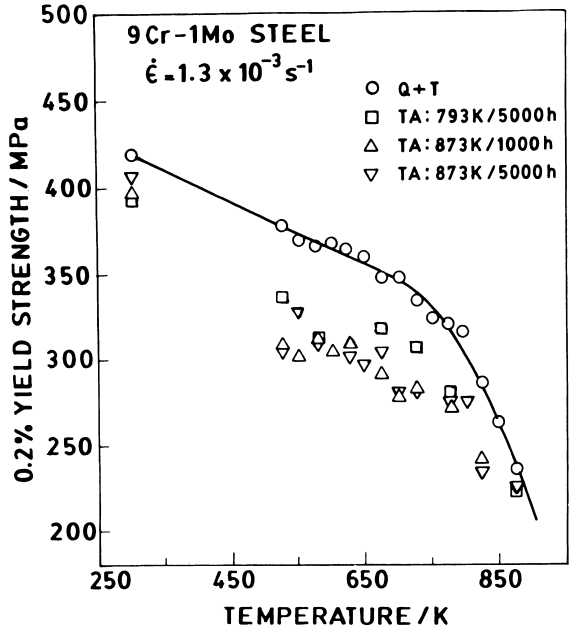

Fig. 7. Influence of prior thermal ageing on yield strength values of 9Cr–1Mo steel at various temperatures.

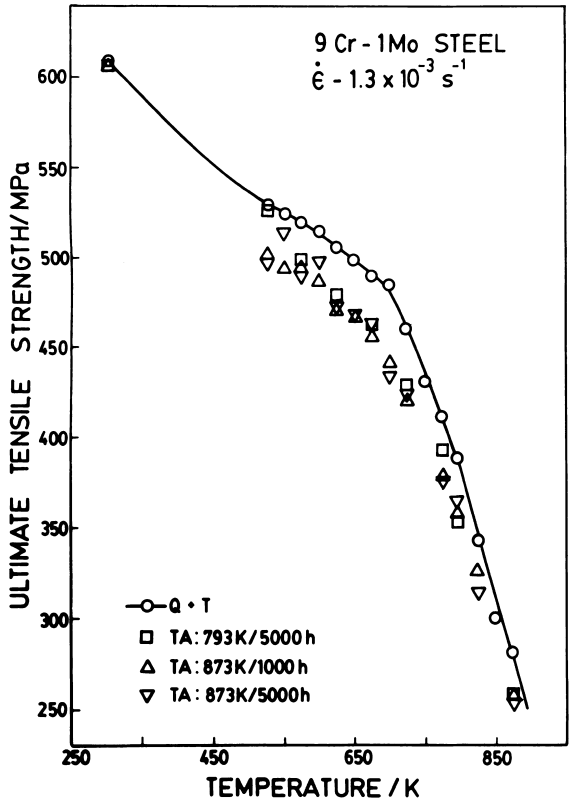

Fig. 8. Influence of prior thermal ageing on ultimate tensile strength of 9Cr–1Mo steel at various temperatures.

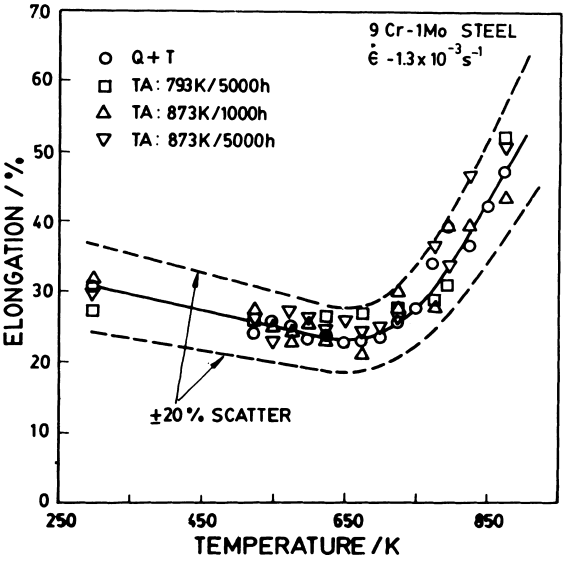

Fig. 9. Influence of prior thermal ageing on elongation to fracture values of 9Cr–1Mo steel at various temperatures.

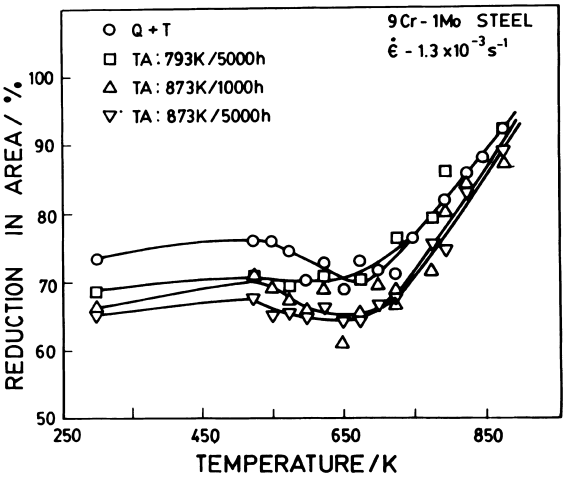

Fig. 10. Influence of prior thermal ageing on reduction in area values of 9Cr–1Mo steel at various temperatures.

the elongation to fracture and reduction in area in Q + T and thermally aged conditions decreased gradually with increasing temperature up to an intermediate temperature followed by a rapid increase at high temperatures.

The average work hardening rate, θ, for all the test conditions was computed as

$$\theta = (\sigma_{0.05} - \sigma_{0.005})/0.045,$$

where $\sigma_{0.05}$ and $\sigma_{0.005}$ refer to the true stress values corresponding to the true plastic strains (ϵ) of 0.05 and 0.005, respectively. Fig. 11 shows variation of θ in Q + T and thermally aged conditions with temperature. θ

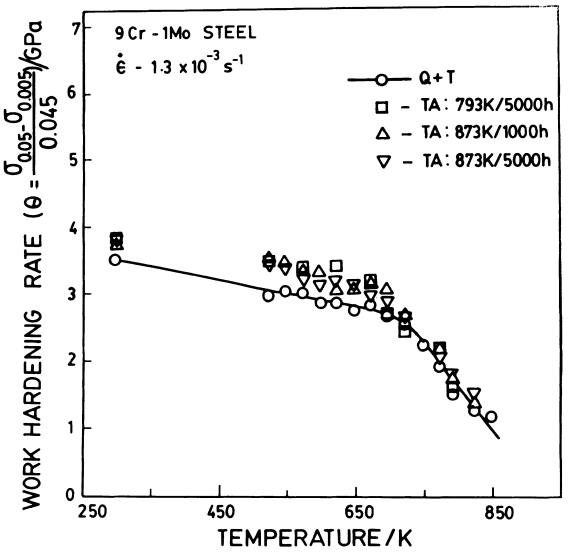

Fig. 11. Variation of average work hardening rate with temperature in 9Cr–1Mo steel in Q + T and thermally aged conditions.

decreased gradually with increasing temperature up to an intermediate temperature followed by a rapid decrease at high temperatures. Further, at room and intermediate temperatures, thermally aged specimens exhibited higher average work hardening rates than that observed in Q + T specimens. A larger reduction in yield strength than in ultimate tensile strength resulted in higher θ values at these temperatures.

The influence of thermal ageing on room temperature strength value of thick section 9Cr–1Mo steel forging is in agreement with those reported for thin sections [11–14]. Wall et al. [11] observed insignificant change in the strength values of normalised and tempered thin section 9Cr–1Mo steel at room temperature due to thermal ageing at 773 and 823 K for durations up to 5000 h. Hippsley and Haworth [12] and Senior et al. [13,14] have also reported similar strength values of specimens in normalised and tempered and thermally aged (at 773 and 873 K for durations up to 5000 h) conditions at room temperature. The similar strength values of Q + T and thermally aged specimens of 9Cr–1Mo steel at room temperature can be viewed in terms of the combined effects associated with solid solution strengthening and precipitation hardening. In the thermally aged condition, increase in the precipitate density, volume fraction and equivalent particle diameter and decrease in mean interparticle spacing [11–14] would lead to enhanced precipitation hardening. Increase in total weight of bulk precipitates after thermal ageing for longer durations at 793 and 873 K observed in the present investigation also suggest increased precipitation due to thermal ageing (Fig. 4). Further, the increased density of precipitates would also cause depletion of solute concentration in the solid solution, which would result in a decreased contribution of solid solution strengthening. Hence, the increase in precipitation hardening compensates the loss of solid solution strengthening upon thermal ageing, so that the total strength remains nearly constant. Wall et al. [11] reported a ductility trough after thermal ageing at 823 K for 1000 h. No such ductility trough was observed at room temperature in the present investigation. The influence of thermal ageing on the room temperature tensile ductility of the forging is in agreement with that reported by Hippsley and Haworth [12], which showed a systematic decrease in the reduction in area with increasing thermal ageing, whereas the elongation to fracture remained largely unaffected.

9Cr–1Mo steel forging in the thermally aged condition has shown a significant reduction in strength values at intermediate temperatures than that observed at high temperatures (Figs. 7 and 8). At intermediate temperatures, the alloy in Q + T and thermally aged conditions exhibited serrated (jerky) flow in the load-elongation curves, a manifestation of dynamic strain ageing (DSA). The segments of various types of serrations observed in Q + T condition are shown in Fig. 12. Careful analysis and comparison of load-elongation curves facilitated distinction between different types of serrations observed during tensile deformation of 9Cr–1Mo steel. These serrations can be classified into A, B or C [18–21]. At the applied strain rate of 1.3×10^{-3} s^{-1}, type A serrations were observed in the low temperature range 523–573 K. Type A serrations occur due to periodic locking of dislocations and show abrupt rises in the load followed by discontinuous drops to or below general level of load-elongation curves. In the temperature range 598–648 K, mixed type A + B serrations were seen. Type B serrations oscillate about the mean load values, i.e., the general level of load-elongation curves. Unlocking type C serrations characterized by load drops always below the general level of load-elongation curves interspersed with type A serrations were observed at 673 K. At the highest temperature of serrated flow at 698 K, only mild irregularities could be seen. These mild irregularities could not be identified with any known type of serrations. Prior thermal ageing (i.e., at 793 K for 5000 h and at 873 K for 1000 and 5000 h) did not exhibit any significant influence on the type of serrations or on the serrated flow temperature range compared to that observed in Q + T condition. Hence, the segments of various types of serrations observed in thermally aged conditions are not shown separately. However, the various types of serrations encountered at different temperatures and heat treatment conditions are summarised in Table 2.

Serrations in load-elongation curves were observed only after the specimens have been deformed beyond a certain strain level, the critical strain (ϵ_c). This critical

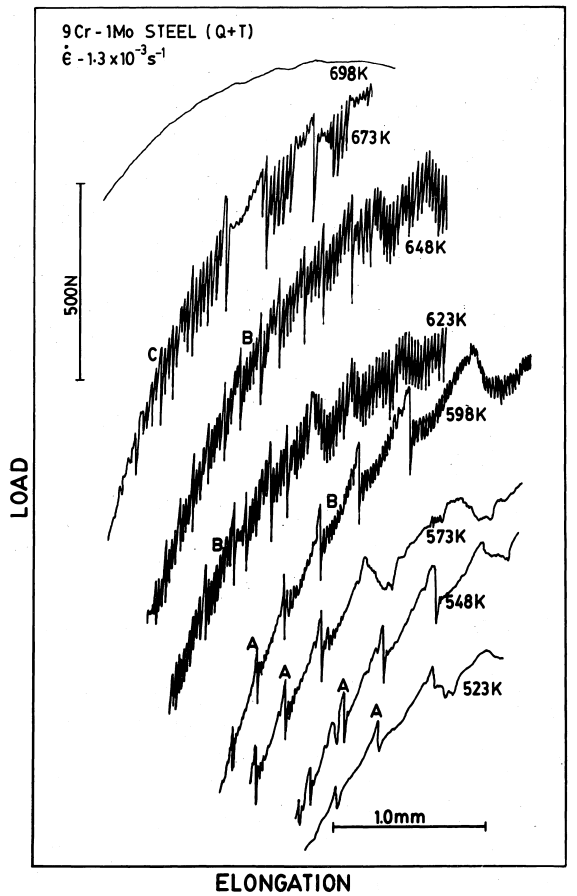

Fig. 12. Segments of typical load-elongation curves obtained for Q + T specimens showing serrated flow at various temperatures at a strain rate of 1.3×10^{-3} s^{-1}.

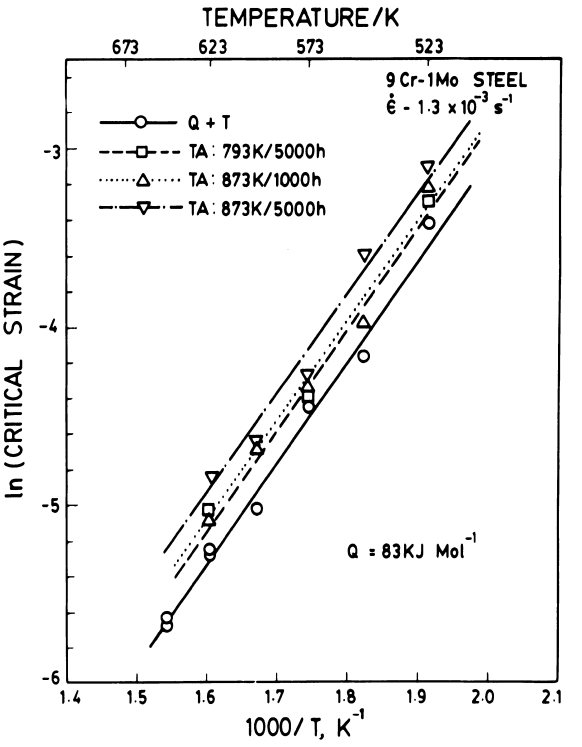

Fig. 13. The temperature (T) dependence of critical strain (ϵ_c) for the onset of serrated flow at a strain rate of 1.3×10^{-3} s^{-1} for Q + T and TA specimens.

strain was found to depend on applied strain rate and temperature. ϵ_c for types A and A + B serrations decreased with decrease in applied strain rate and an increase in test temperature (e.g., influence of temperature on ϵ_c in Fig. 13). Thermally aged specimens displayed two important differences compared to Q + T specimens. Firstly, the critical strain for the onset of serrations increased with increasing thermal ageing (Fig. 13). However, the strain rate and temperature dependences of critical strain and apparent activation energy value remained similar to that observed in Q + T condition. The determination of apparent activation energy for serrated flow has been described in detail in Ref. [22]. An apparent activation energy of 83 kJ mol^{-1} has been obtained [22]. This value of activation energy suggested that the diffusion of interstitial solute such as carbon is responsible for DSA in the alloy. Secondly, the height of serrations, i.e., the magnitude of stress drops ($\Delta\sigma$) observed during serrated flow decreased with increasing thermal ageing. A summary of the magnitude of stress drops at a plastic strain of 4% for type A serrations in Q + T and thermally aged specimens is presented in Table 3. At all temperatures, a systematic decrease in the value of stress drops with increase in temperature and duration of thermal ageing could be seen in Table 3.

Table 2
Type of serrations in Q + T and thermally aged specimens tested at a strain rate of 1.3×10^{-3} s^{-1} at various temperatures

Heat treatment condition	Type of serrations at temperatures (K)						
	523	548	573	598	623	648	673
Q + T	A	A	A	A + B	A + B	A + B	A + C
TA: 793 K/5000 h	A	–	A	–	A + B	–	A + C
TA: 873 K/1000 h	A	A	A	A + B	A + B	A + C	A + C
TA: 873 K/5000 h	A	A	A	A + B	A + B	A + C	A + C

Table 3
Magnitude of stress drop ($\Delta\sigma$) at a plastic strain of 4% for type A serration in Q + T and thermally aged specimens tested at a strain rate of 1.3×10^{-3} s^{-1} at various temperatures

Heat treatment condition	Stress drop ($\Delta\sigma$/MPa) at temperatures (K)						
	523 [a]	548	573	598	623	648	673
Q + T	7.0	8.9	15.0	16.4	18.9	20.9	23.3
TA: 793 K/5000 h	2.9	–	11.9	–	15.5	–	12.6
TA: 873 K/1000 h	5.0	6.4	10.7	13.1	15.5	15.6	16.0
TA: 873 K/5000 h	1.6	4.3	9.7	12.2	14.9	14.9	12.6

[a] Stress drop at 523 K corresponds to plastic strain of 5%.

Further, Table 3 also shows a general increase in stress drop with increasing test temperature in both Q + T and thermally aged conditions. Decrease in the height of serrations or stress drops indicates reduced strength of solute locking of dislocations, whereas increase in the critical strain implies delay in the formation of effective solute atmosphere to lock the dislocations and the onset of serrated flow. Both these observations indicate reduced propensity to DSA due to thermal ageing in 9Cr–1Mo steel. The reduced propensity to DSA has been ascribed to the increased precipitate sinks (i.e., increased density of carbides) as well as reduced carbon concentration in the solid solution due to thermal ageing [22]. The decreased propensity to DSA has resulted in a significant reduction in strength values at intermediate temperatures.

The variation of ductility with increasing temperature observed in Q + T and thermally aged specimens of the forging (Figs. 9 and 10) is in agreement with that reported for thin section 9Cr–1Mo steel in normalised and tempered condition [2] and in the thick section forging in simulated post weld heat treatment condition [7,8]. Similar variation in ductility with temperature has also been reported for modified 9Cr–1Mo steel in normalised and tempered condition [23]. The fracture mode in Q + T and thermally aged conditions remained transgranular ductile at all test conditions investigated. Q + T specimens exhibited ductile fracture characterized by dimples resulting from coalescence of microvoids (Fig. 14). On the other hand, specimens aged for durations of 500 h and more exhibited chisel fracture at room and intermediate temperatures (Fig. 15) along with microvoid coalescence. The propensity toward chisel fracture could have occurred by split in the lath boundaries to produce individual stringers, which fail by shear and gave a chisel tip appearance on the fracture surface. The chisel fracture has been found to increase with increasing thermal ageing. Hippsley and Haworth [12] observed chisel fracture in thin section 9Cr–1Mo steel thermally aged at 773 and 873 K for durations of 1000 and 5000 h. Jordan et al. [24] reported some amount of chisel fracture along with microvoid coalescence in 9Cr–1Mo steel thermally aged at 823 K for 5000 h. The chisel fracture was promoted by the presence of higher amounts of silicon and phosphorous in the aged alloy. The occurrence of chisel fracture in the aged specimens has been ascribed to the presence of brittle Laves phase, promoting martensite lath boundary split [12,24]. It was pointed out that the phosphorous which segregates to lath and grain boundaries in the as-tempered condition is progressively taken into the solution in Laves phase during ageing. Hence, phosphorous is an important but a secondary factor in the embrittlement process in this steel [12]. Senior et al. [14] reported a significant reduction in the interfacial strength of $M_{23}C_6$ carbides after ageing at 823 K for 1000 h due to segregation of phosphorous to carbide/matrix interface. At longer ageing time of 5000 h, phosphorous gets incorporated into the solution of Fe_2Mo partially and, therefore, provides the dominant site for void nucleation [14]. The larger decrease in the reduction in area at room and intermediate temperatures due to thermal ageing observed in this investigation (Fig. 10) can be attributed to the occurrence of relatively less ductile chisel fracture in the forging (Fig. 12). Brittle intergranular or mixed mode of ductile/brittle intergranular fracture reported by Wall et al. [11] in the ductility trough region in the

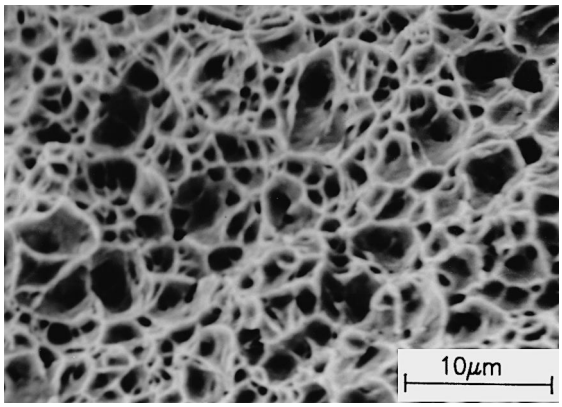

Fig. 14. SEM fractograph showing transgranular fracture in Q + T specimen tested at 793 K at a strain rate of 1.3×10^{-3} s^{-1}.

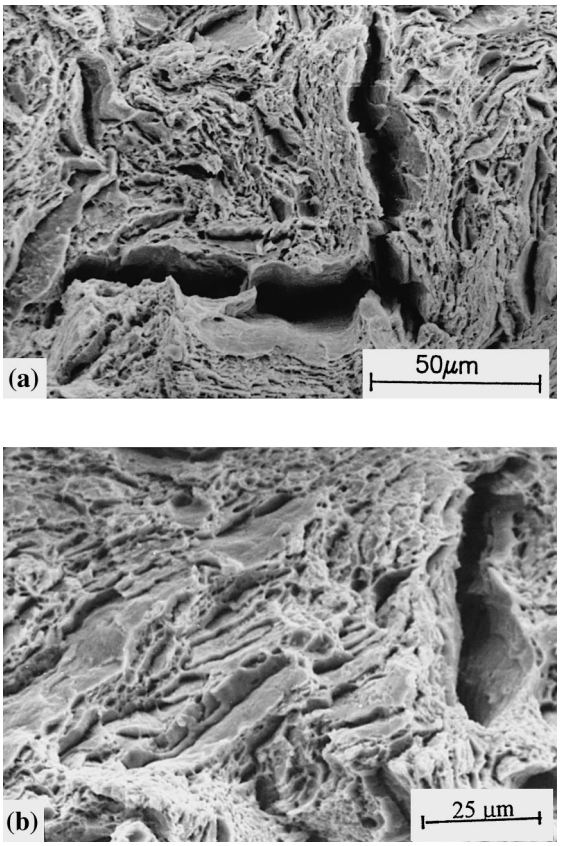

Fig. 15. SEM fractographs showing transgranular fracture with chisel tip appearance at: (a), 300 K and (b), 573 K in thermally aged (873 K/5000 h) specimens tested at a strain rate of 1.3×10^{-3} s^{-1}.

thin section thermally aged 9Cr–1Mo steel has not been observed in the thermally aged specimens of the forging in the present investigation. At high temperatures, thermally aged specimens failed by transgranular fracture characterized by dimples similar to that observed in Q + T specimens.

4. Conclusions

The yield and ultimate tensile strengths of 9Cr–1Mo tube plate forging at room temperature were little affected by prior thermal ageing at 793 and 873 K for durations in the range 10–5000 h. Thermal ageing for longer durations at 793 K (5000 h) and 873 K (1000 and 5000 h) results in a significant reduction in strength values at intermediate temperatures. The reduction in strength values at intermediate temperatures can be ascribed to the reduced propensity to dynamic strain ageing arising from increased precipitate sinks (i.e., increased density of carbides) as well as decreased carbon concentration in the solid solution due to thermal ageing.

The elongation to fracture remained largely unaffected by thermal ageing at all temperatures and the values remained within 20% scatter band for Q + T specimens. The reduction in area was found to decrease consistently with increasing thermal ageing at all temperatures. The fracture mode remained transgranular ductile at all test conditions. Q + T specimens exhibited dimples on the fracture surface resulting from microviod coalescence. At room and intermediate temperatures, specimens aged for longer durations exhibited chisel fracture resulting from a split in the lath boundaries. The influence of prior thermal ageing on room temperature tensile properties remained similar to that observed for thin section 9Cr–1Mo steel.

Acknowledgements

Authors are thankful to Dr. Placid Rodriguez, Director and Dr. Baldev Raj, Group Director, Metallurgy and Materials Group, Indira Gandhi Centre for Atomic Research, Kalpakkam, for their keen interest in this work.

References

[1] B.J. Cane, R.S. Fiddler, in: Proceedings of the International Conference on Ferritic Steels for Fast Reactor Steam Generators, London, 1977, p. 193.
[2] D.S. Wood, A.B. Baldwin, F.W. Grounds, J. Wynn, E.G. Wilson, J. Waring, in: Proceedings of the International Conference on Ferritic Steels for Fast Reactor Steam Generators, London, 1977, p. 189.
[3] D.S. Wood, A.B. Baldwin, K. Williamson, in: Proceedings of the IAEA Meeting on Time and Load Dependent Degradation of Pressure Boundary Materials, Innsbruck, Austria 1978, Report IWG-RRPC-79/2, 1979, p. 88.
[4] E. Barker, G.J. Lloyd, R. Pilkington, Mater. Sci. Eng. 84 (1986) 49.
[5] J. Orr, S.J. Sanderson, in: Proceedings of the Topical. Conference on Ferritic Alloys for use in Nuclear Energy Technologies, AIME, New York, 1983, p. 261.
[6] S.J. Sanderson, S. Jacques, in: Proceedings of the IAEA Specialist Meeting on Mechanical Properties of Structural Materials Including Environmental. Effects, Chester, England 1983, Report IWGFR-49, vol. 2, 1984, p. 601.
[7] B.K. Choudhary, Ph.D. Thesis, Indian Institute of Technology, Bombay, India, 1997.
[8] B.K. Choudhary, K. Bhanu Sankara Rao, S.L. Mannan, Int. J. Pres. Ves. Piping 58 (1994) 151.
[9] B.K. Choudhary, S.K. Ray, K. Bhanu Sankara Rao, S.L. Mannan, BHM (Berg und Heuttemmaennische Monatshafte) 137 (1992) 439.
[10] K. Laha, K.S. Chandravathi, K.B.S. Rao, S.L. Mannan, Int. J. Pres. Ves. Piping 62 (1995) 303.

[11] M. Wall, B.C. Edwards, J.A. Hudson, in: Proceedings of the Specialist Meeting on Mechanical Properties of Structural Materials including Environmental Effects, Chester, UK, 1983, Report IWGFR-49, vol. 2, 1984, p. 545.
[12] C.A. Hippsley, N.P. Haworth, Mater. Sci. Technol. 4 (1988) 791.
[13] B.A. Senior, F.W. Noble, B.L. Eyre, Acta Metall. 34 (1986) 1321.
[14] B.A. Senior, F.W. Noble, B.L. Eyre, Acta Metall. 36 (1988) 1855.
[15] C.R. Brinkman, B. Gieseke, P.J. Maziasz, in: P. K. Liaw et al. (Ed.), The Minerals, Metals and Materials Society, 1993, p. 107.
[16] W.B. Jones, Ferritic steels for high temperature applications, in: A.K. Khare (Ed.), ASM International, Metals Park, Ohio, 1984, p. 221.
[17] S. Saroja, P. Parmeshwaran, M. Vijaylakshmi, V.S. Raghunathan, Acta Metall. Mater. 43 (1995) 2985.
[18] B. Russel, Philos. Mag. 8 (1963) 615.
[19] C.F. Jeskins, G.V. Smith, Trans. Metall. Soc. AIME 245 (1969) 2149.
[20] A.J.R. Solar Gomez, W.J. Mc Tegart, Philos. Mag. 20 (1969) 495.
[21] P. Rodriguez, Bull. Mater. Sci. 6 (1984) 653.
[22] B.K. Choudhary, K. Bhanu Sankara Rao, S.L. Mannan, B.P. Kashyap, Serrated yielding in 9Cr–1Mo ferritic steel, Mater. Sci. Technol., in press.
[23] V.K. Sikka, M.G. Cowgil, B.W. Roberts, in: Proceedings of the Topical. Conference on Ferritic Alloys for Use in Nuclear Energy Technologies, AIME, New York, 1993, p. 317.
[24] G.R. Jordan, S.J. Andrews, C.A. Hippsley, Mater. Sci. Technol. 9 (1993) 1115.